International Journal of Mechanical and Production Engineering Research and Development (IJMPERD)
ISSN (P): 2249–6890; ISSN (E): 2249–8001
Vol. 10, Issue 3, Jun 2020, 1165-1176

TRANS STELLAR
•Journal Publications •Research Consultancy

INFLUENCE OF PROCESS PARAMETER ON THE HEIGHT DEVIATION OF WELD BEAD IN WIRE ARC ADDITIVE MANUFACTURING

NOR ANA ROSLI[1], MOHD RIZAL ALKAHARI[2], FAIZ REDZA RAMLI[3] & MOHD FADZLI ABDOLLAH[4]

[1,4]*Faculty of Mechanical Engineering, Universiti Teknikal Malaysia Melaka, Malaysia*

[2]*Advanced Manufacturing Center, Universiti Teknikal Malaysia Melaka, Malaysia*

[3]*Centre for Advanced Research on Energy, Universiti Teknikal Malaysia Melaka, Malaysia*

ABSTRACT

Significant attention towards Wire and Arc Additive Manufacturing (WAAM) has gradually increased. WAAM technology has been proven in building three-dimensional (3D) metal parts efficiently and economically. The combination of wire and arc welding is promising, especially in depositing metals with higher deposition rate, and low cost of raw materials, as well as manufacturing of a large-scale product. However, there are several process parameters should be optimized to ensure no internal defect, acceptable surface finish and consequently to have a good quality of final parts when using WAAM. Therefore, an experimental design using the Taguchi method was used to determine the effect of welding current, welding voltage, and travel speed on the responses, including the deviation in height were investigated. The results revealed that travel speed was the dominant factor affecting the waviness surface structure on top of the 3D metal parts. Besides, the contribution rate for each factor to the deviation in height was also determined.

KEYWORDS: Wire Arc Additive Manufacturing, Gas Metal Arc Welding, 3D Printing, Additive Manufacturing & Advanced Manufacturing

Received: May 15, 2020; **Accepted:** Jun 05, 2020; **Published:** Jun 26, 2020; **Paper Id.:** IJMPERDJUN2020101

Original Article

1. INTRODUCTION

Additive Manufacturing (AM) has continually developed over the last three decades, from prototype application to production parts (Michel et al., 2019; Xu et al., 2018). The increasing demands of this technology has motivated many researchers to focus on refining the quality of AM parts (Brandl et al., 2010; Müller et al., 2019). Among the industries looking forward to this technology are automobile and aerospace industries. Wire and Arc Additive Manufacturing (WAAM) is one of the options among numerous technologies in AM that can be used build 3D metal parts. Indeed, WAAM is an emerging manufacturing technology and has several technical issues that must be overcome (J. L. Z. Li et al., 2019). Commonly, AM process is mainly used to fabricate 3D metal parts, such as selective laser melting (SLM), Electron Beam Melting (EBM) and Direct Metal Deposition (DED)(Park et al., 2016).

WAAM technology utilizes electric arc welding as the heat source and a metal wire as the feedstock material. The conventional arc welding mainly used in WAAM is Gas Metal Arc Welding (GMAW)(J. Ding et al., 2011), Gas Tungsten Arc Welding (GTAW) (Dickens et al., 1992), and Plasma Arc welding (PAW) (Spencer et al., 1998). WAAM technology is applied to fabricate parts by depositing metals in the form of the layer-by-layer process (Y. Li et al., 2018; Rodrigues et al., 2019). During the process, the heat source increases with increasing layer height and continues until the model is complete. Currently, WAAM is being used by both academia and

industry fields due to its advantages. The research related to WAAM deals with the fundamental aspect of process parameters and material properties. The process parameters are challenging to be determined as well as to understand their characteristics and response on the metal deposited. According to (Rodrigues et al., 2019), the optimal selection of parameters is crucial and affects the transfer mode. (D. Ding et al., 2014) explored the optimal build path for stable deposition and the desired properties of components. The build path planning is based on the effect of the thermal process in deposited metals to geometrical features. (Xiong et al., 2018) proposed the viewing of surface appearance of the parts deposited using a laser vision system for a better understanding on the influence of process parameters on surface roughness. In addition, to detecting the presence of defects without altering the static properties of the specimen, (Astarita et al., 2019) used Computed Tomography (CT) to detect defects and voids. The aim was to interact with the mechanical properties of WAAM in order to understand the limiting factors.

However, the lack of understanding of the process parameters limits the extensive application of WAAM. Indeed, WAAM has a vast number of process parameters, and involves a complex relation that is intertwined. Currently, researchers rarely emphasize on the deviation in the height, as the essential response on the process parameters. The deviation in the height is introduced due to the uneven weld bead geometry that occurs at the start and end point of welding pass. (D. Ding et al., 2014), proposed a minimum number of tool-path element in order to reduce the effect of starting and stopping and cumulative deviation overlap. Thus, this study aims to understand the influence of three process parameters, namely welding current, welding voltage, and travel speed on the deviation in the height of weld bead geometry, and to optimize the factors by investigating acceptable geometries by using the Taguchi statistical method.

2. EXPERIMENTAL PROCEDURES

2.1 Sample Fabrication

The set-up of the WAAM system employed for this study is shown in Figure 1. The WAAM system consists of a GMAW unit with a wire material (ER308LSi), of 0.8 mm in diameter as a filler material. All the samples were fabricated on top surface of a mild steel base plate of 200 mm × 200 mm × 6 mm that were set as substrate material. The element composition of welding wire was characterized using energy dispersive spectrometer (EDS) as shown in Table 1. An in-house developed 3D metal printer was used throughout the study (Rosli et al., 2018), whereby the GMAW welding torch was installed perpendicular on the substrate. The wire feed as the filler material was coaxial along the GMAW unit.

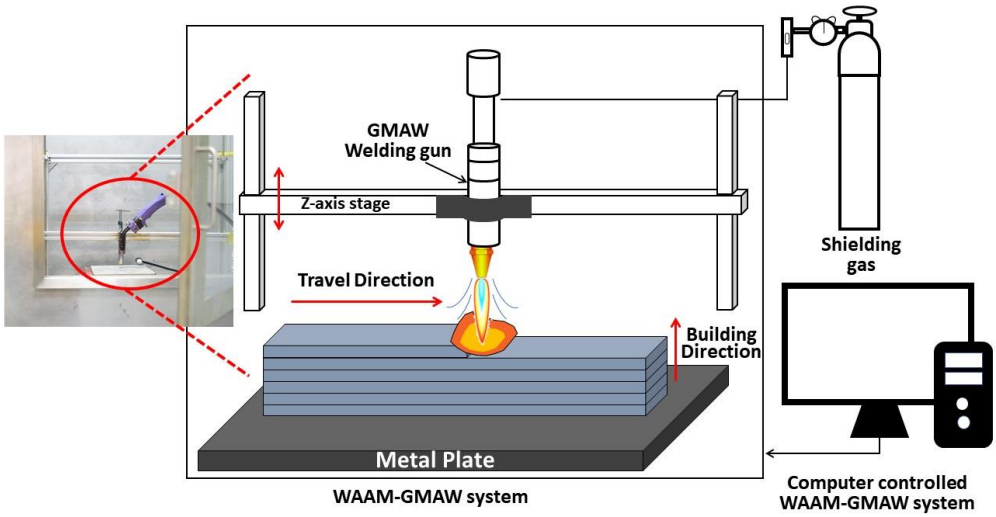

Figure 1: Schematic diagram of WAAM-GMAW system

Table 1: Element composition of welding wire (wt %)

Element	C	Cr	Fe	Ni
Stainless steel 304	2.83	14.33	79.31	3.53

The schematic of deposition direction, as shown in Figure 2 indicates the travel direction of deposition and positioning of the welding torch and substrate. The deposition direction is zig zag where each layer is in reverse direction to avoid height difference between the start and stop regions. The sample dimensions of multilayer deposition of 120 mm length, 40 mm height, and 5 mm width were fabricated on top of the substrate. The actual view of the arc welding torch and 3D metal printer before during deposition are shown in Figure 2. The typical process involved slicing the parts into the layer, converting to g-code file, and building physical parts.

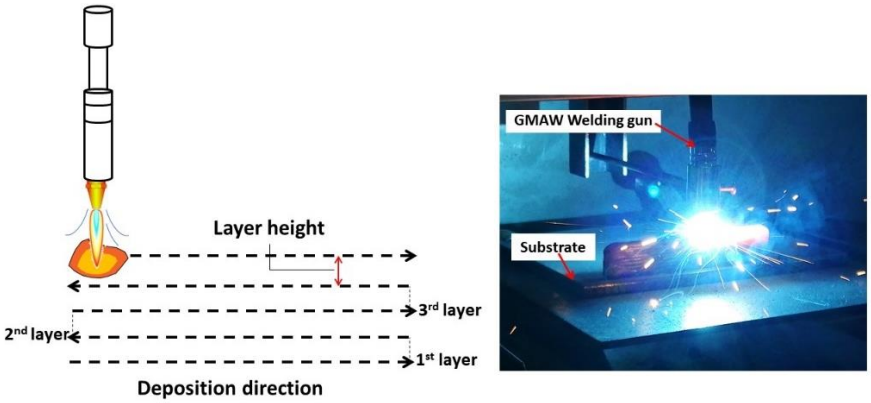

Figure 2: Schematic of deposition tool path direction.

2.2 Deviation in Height Measurement

The sample was fabricated from Computer Aided Design (CAD) on the top surface of the mild steel plate. The deviation in height is the surface waviness resulting from the parts deposited by GMAW based on AM. The effect of bead height deviation disrupted where the multilayers overlapped, but could be observed clearly on the top of layers. (Duraisamy et al., 2019) produce the WAAM process plate and the waviness was removed by machining in order to prepare the final sample size. This due to the uneven layer surface that may lead to unstable deposition. The deviation in height was measured using Coordinating Measuring Machine (CMM) along the top surface of the wall and the root mean square error of height deviation was calculated as the representative parameters. The schematic of geometrical measurement for deviation in height is shown in Figure 3.

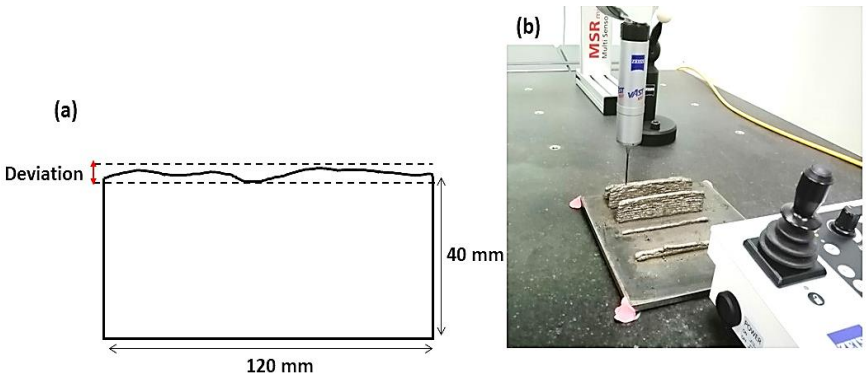

Figure 3: (a) Geometrical Measurement of Deviation in Height, (b) Coordinate Measuring Machine (CMM) Measured along with the Height on top of the wall.

2.3 Experimental Design and Optimization

The design of experiment using the Taguchi method is a powerful technique that can identify the best combination of factors and parameters with limited information. This method has been widely used to minimize the number of tests using orthogonal arrays and reduce the effect of the cause with regard to the performance and quality. By using the technique, calculation of the loss function between the deviation and desired value can be performed through which the value of Signal to Noise (S/N) ratio can be obtained. The calculation of S/N ratio for each level of process parameter is based on the quality characteristics in the analysis of S/N. Basically, there are three S/N analysis available in representing the quality: the lower-the-better, the higher-the-better, and the nominal-the-best (Gupta et al., 2011; Mandal et al., 2011). Since this study aims to minimize the deviation in height or waviness of the top surface, therefore the lower-the-better characteristic was used, as shown in equation (1):

$$S/N = -10 \log \text{ (mean of sum of square measured data)}$$

$$S/N = -10 \log \left[\frac{1}{n}\sum_{i=1}^{n} y_i^2\right] \quad (1)$$

Where y_i is the value of the response obtained, i is the repetition of the trial, and n is the number of repetitions of each trial (Mandal et al., 2011). Next, the Analysis of Variance technique (ANOVA) was performed to find if either the process factor is statistically significant or insignificant and to calculate their contribution rate. These ranges of input parameters were chosen based on preliminary research, as shown in Table 2. Three factors were selected for consideration: welding current, welding voltage and travel speed. Each factor has three-levels, as shown in Table 3. The start and endpoints of deposition are similar for all samples.

Table 2: Processing Parameters

Parameters	Unit	Range
Wire material		ER308LSi
Wire diameter	mm	0.8
Current, I	A	85, 95, 105
Voltage, V	V	17, 17.5, 18.1
Travel speed	mm/s	4, 5, 6
Layer height	mm	2
Stand of distance	mm	5

3. RESULTS AND DISCUSSIONS

3.1 Analysis of the S/N Ratio

The deviation in the height was determined for all possible combinations using the Taguchi technique in order to optimize the control process parameters. The experimental layout with the L9 orthogonal array was used because there are three-factors and three-levels in this experiment, (i.e., $L_9(3^3)$) as shown in Table 4. Each combination of process parameter controls the response of standard deviation of height. The lower the deviation in the height represents the best combination of process parameters in generating regular and smooth track geometry. The equation used to calculate the S/N ratio and to observe the response factor is the lower-the-better option.

Table 3: Process Parameter WAAM and their Levels

Control Factor	Symbol	Levels		
		1	2	3
Current (A)	A	85	95	105

Voltage (V)	B	17.0	17.5	18.1
Travel speed (mm/s)	C	4	5	6

Table 4: Orthogonal Array of Taguchi, L9(33)

Experiment run	A	B	C
1	1	1	1
2	1	2	2
3	1	3	3
4	2	1	2
5	2	2	3
6	2	3	1
7	3	1	3
8	3	2	1
9	3	3	2

The result of surface waviness is plotted in the graph and is shown in Figure 4. Based on observation, the surface waviness on the top of parts is uneven for all samples. The desired height is 40 mm. After deposition, the samples obtained the total height around 28.884 to 33.246 mm for each sample. The reduction in height occurred due to continuous deposition and reduced cooling rate. According to(Ryan, 2018), the significant difference in dimension between the actual process and desired is due to the layer height, cooling time between layers, and direction of tool path that influences deposition and solidification of the material. However, this study focuses on the deviation in height after solidification and the main contribution process parameter affected, such as welding current, welding voltage and travel speed of the 3D metal printer.

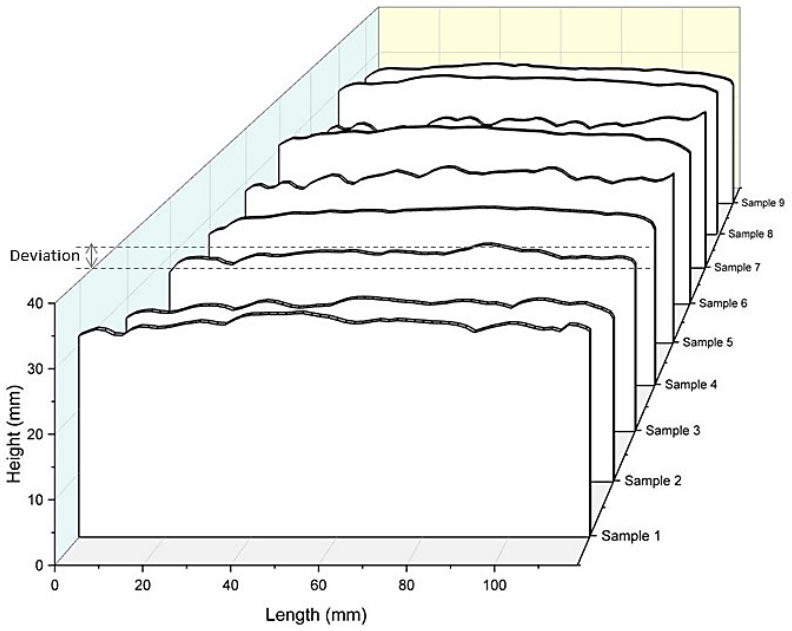

Figure 4: The Waviness on Top of sample along Deposited.

The results of experiment obtained are as shown in Table 5. The average computation value of the deviation in height is 0.857957 mm. Similarly, the average computation value of the S/N ratio is 2.814714 db. After calculating the average values of the S/N ratio for each level, the S/N ratio can be similarly computed for each factor, as presented by the response shown in Table 6.

The response table of S/N ratio indicates the optimal level of input factor for the optimal deviation in height. The optimal parameters for minimizing the height deviation can be easily determined from Table 6 and Figure 5 graph. The optimum parameters for control factor A, B, and C corresponds to the highest value of S/N ratio in each level. Based on the results of response table, the optimal parameters that give acceptable height deviation value for control factor A, B, and C are level 3; (S/N = 2.1861), level 3; (S/N = 2.2385), and level 2; (S/N =2.4683), respectively. In other words, the S/N ratio that represents the optimum height deviation exists at the current of 105 A, voltage of 18.1 V and travel speed of 5 mm/s. The ranking of important parameters based on the delta value shows that travel speed is in the first rank, followed by welding current and welding voltage.

Table 5: The Results of Experiments and S/N Ratio Values

Experiment run	Control Factor			Height deviation (mm)	S/N ratio(db)
	Current (A) A	Voltage (V) B	Travel Speed (mm/s) C		
1	85	17	4	0.90543	0.86290
2	85	17.5	5	0.69256	3.19085
3	85	18.1	6	0.83930	1.52166
4	95	17	5	0.94638	0.47869
5	95	17.5	6	1.11504	-0.94581
6	95	18.1	4	0.84545	1.45824
7	105	17	6	1.01583	-0.13642
8	105	17.5	4	0.71127	2.95931
9	105	18.1	5	0.65047	3.73545

Table 6: S/N Ratio Response Table for Height Deviation Factor

Level	Control Factor		
	A	B	C
1	1.8585	0.4017	1.7602
2	0.3304	1.7348	2.4683
3	2.1861	2.2385	0.1465
Delta	1.8557	1.8367	2.3219
Rank	2	3	1

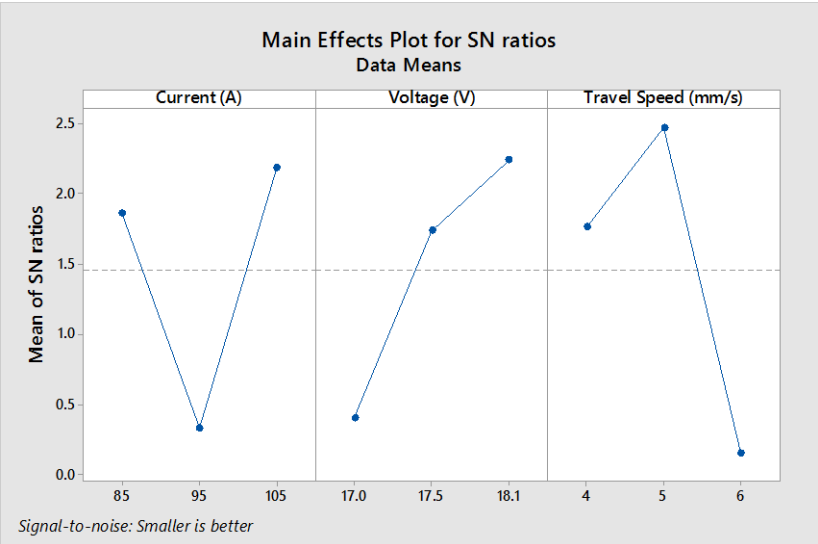

Figure 5: Main Effects Plot for S/N Ratio

3.2 Effects of Process Parameters

The contour plot, as seen in Figure 6, shows the interaction between dependent and independent variation. This plot depicts the model regression equation and the set of parameters used to achieve the minimum deviation in the height. As shown in equation (2), the regression equation is obtained to predict the outcome variable. The darker area indicates the highest deviation in the height value. Figure 6(a) displays the contour plot of the current-voltage relationship used to produce the 3D model and the range of deviation in the height. The current and voltage at the intermediate level reached the highest height deviation above 1.1 mm, while the higher current and higher voltage levels would reduce the height deviation below 0.7 mm. In general, high welding current is the mandatory and inevitable cause of excessive heat input (Liu et al., 2019). Welding current at 95 A resulted in the highest deviation in the height because the heat input and metal deposition rate increased with the current increase (Samir Khan et al., 2018). Nonetheless, these problems can be solved by controlling certain input parameter combinations, such as voltage and velocity.

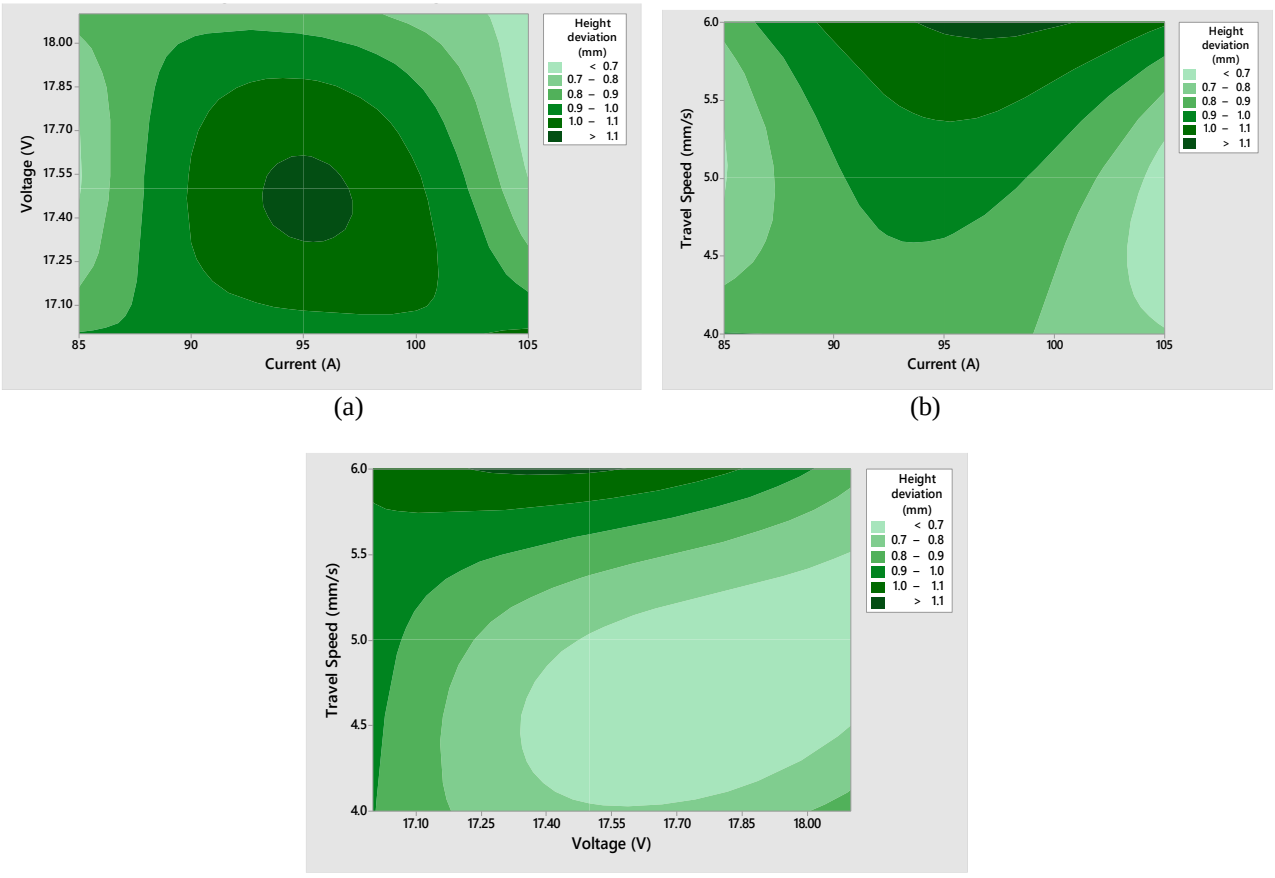

Figure 6: Contour Plot with respect to Height Deviation (mm) (a) Voltage (V) and Current (A), (b) Travel speed (mm/s) and Current (A), and (c) Travel Speed (mm/s) and Voltage (V)

The contour plot in Figure 6(b) shows the higher travel speed levels and lower voltage levels generating highest deviation in the height value and vice versa for lower deviation in the height value. The increased voltage created results in an increase in bead width and a slight decrease in bead height. Thus, it contributes to high heat input and a slow cooling rate during the deposition of WAAM (Seow et al., 2019). Figure 6(c) shows the contour plot, as speed increases, the deviation in the height also increases, and this coincides to the voltage and current instability.

The minimization of deviation in the height with an increase in speed, and the controllable voltage arc and current may produce greater stability of the arc generated. Therefore, the optimization of the process consists of the output with minimizing deviation in the height. In order to optimize the deviation in the height, the option selected in the S/N is the lower-the-better option, where the minimization of deviation in height is required. The optimum height deviation, according to S/N calculation, is the current of 105 A, voltage of 18.1 V, and travel speed of 5 mm/s.

3.3 Analysis of Variance Method

ANOVA was used to determine the significant parameters affecting the deviation in height. The method was applied to analyse the effect of welding current, welding voltage and travel speed. Furthermore, the analysis was carried out to find the contribution of each factor and a higher contribution rate on the deviation in height. As shown in Table 7, the contribution of control factors A, B and C is 28.95%, 25.20% and 43.14% respectively. Travel speed recorded the highest percentage of contribution rate on the deviation in height with 43.14%. According to the ANOVA result, the percentage of error was considerably low at 2.71% for the deviation in height.

Table 7: Result of ANOVA for Deviation in Height

Variance source	Degree of freedom (DoF)	Sum of squares (SS)	Mean square (MS)	F ratio	Contribution rate (%)
A	2	0.056026	0.028013	10.68	28.95
B	2	0.048760	0.024380	9.29	25.20
C	2	0.083484	0.041742	15.91	43.14
Error	2	0.005247	0.002623	-	2.71
Total	8	0.193516	-	-	100.00

3.4 Regression Analysis of Height Deviation

The regression analysis was used to establish the relationship between the dependent and independent variable. In this study, the dependent variables are the height deviation, whereas the independent variable is input process parameters, (i.e., current, voltage and travel speed). The regression equation is obtained for the estimation of the height deviation, as shown in equation (2). This equation used to define the height deviation of any parameters within the working input range with a relatively small amount of error. The R-squared value is 46.43%. This value shows that dependent variables can explain 46.43% of the data variance. However, the value may improve by increasing the predictor or independent variables.

$$\text{Height deviation} = 3.32 - 0.00100\ \text{Current (A)} - 0.159\ \text{Voltage (V)} + 0.0847\ \text{Travel speed (mm/s)} \quad (2)$$

3.5 Confirmation Test

The confirmation test is the last step in the Taguchi method to validate the optimal value. The test sample fabricated using the optimal condition of process parameters as mentioned previously, (i.e., current 105 A, voltage 18.1 V, and travel speed 5 mm/s). Table 8 shows a comparison of the test results and the predicted values obtained by the regression equation. From observation, the parts showed minimal deviation in the height and less waviness. The actual test result and predicted value for height deviation gain of 0.65047 mm and 0.7606 mm, respectively. According to (Cetin et al., 2011), for robust statistical analysis, the error values must be less than 20%.

Table 8: Predicted Values and Confirmation Test by Regression Equations

Current (A)	Voltage (V)	Travel Speed (mm/s)	Height deviation (mm)	Predicted	Error (%)
105	18.1	5	0.65047	0.7606	16.93

By comparing all three-confirmation samples, all the parts geometry are very close to each other. As illustrated in Figure 7, the view from the front, top and side of the sample fabricated for the confirmation test

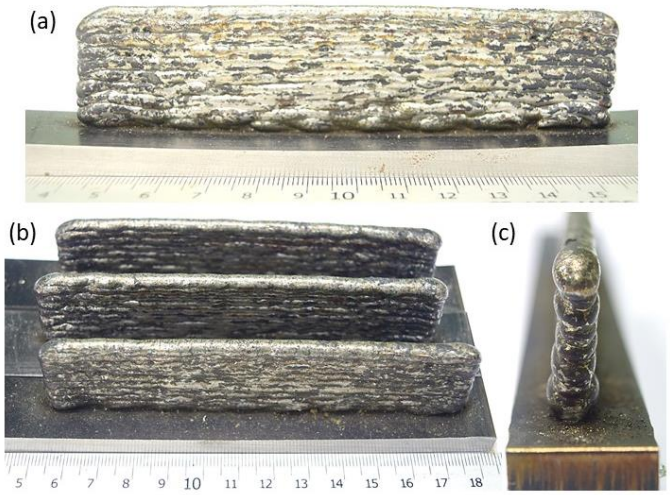

Figure 7: Front, Top and Side view of Confirmation Samples Fabricated.

4. CONCLUSIONS

In this study, an optimal process parameter of WAAM process is determined using the Taguchi method. Based on the S/N ratio response table, the optimal combination for optimizing the deviation in height are 105 A, 18.1 V and 5 mm/s for the welding current, welding voltage and travel speed respectively. The most significant contribution rate among the process parameter in reducing the waviness surface in height is the travel speed with 43.13%. The optimal condition has successfully demonstrated the confirmation test. However, as a recommendation, further studies should consider the geometrical accuracy between the desired and the actual result obtained, as well as the influence of other factors such as temperature, angle of the welding torch, and the incremental height between the layers.

ACKNOWLEDGEMENT

The authors acknowledge the financial support from Zamalah Scheme, Universiti Teknikal Malaysia Melaka.

REFERENCES

1. *Astarita, A., Campatelli, G., Corigliano, P., Epasto, G., Montevecchi, F., Scherillo, F., & Venturini, G. (2019). Microstructure and mechanical properties of specimens produced using the wire-arc additive manufacturing process. Proceedings of the Institution of Mechanical Engineers, Part C: Journal of Mechanical Engineering Science,0954406219883324.*
2. *Brandl, E., Baufeld, B., Leyens, C., & Gault, R. (2010). Additive manufactured Ti-6A1-4V using welding wire: Comparison of laser and arc beam deposition and evaluation with respect to aerospace material specifications. Physics Procedia, 5(Pt 2), 595–606.*

3. Cetin, M. H., Ozcelik, B., Kuram, E., & Demirbas, E. (2011). Evaluation of vegetable based cutting fluids with extreme pressure and cutting parameters in turning of AISI 304L by Taguchi method. Journal of Cleaner Production, 19(17–18), 2049–2056.

4. Devireddy, K. R. I. S. H. N. A. J. A., et al. "Analysis of the influence of friction stir processing on gas tungsten arc welding of 2024 aluminum alloy weld zone." Int. J. Mech. Prod. Eng. Res. Dev 8.1 (2018): 243-252.

5. Dickens, P. M., Pridham, M. S., Cobb, R. C., Gibson, I., & Dixon, G. (1992). Rapid prototyping using 3-D welding. Solid Freeform Fabrication Proceedings, 280–290.

6. Ding, D., Pan, Z., Cuiuri, D., & Li, H. (2014). A tool-path generation strategy for wire and arc additive manufacturing. International Journal of Advanced Manufacturing Technology, 73(1–4), 173–183.

7. Ding, J., Colegrove, P., Mehnen, J., Ganguly, S., Almeida, P. M. S., Wang, F., & Williams, S. (2011). Thermo-mechanical analysis of Wire and Arc Additive Layer Manufacturing process on large multi-layer parts. Computational Materials Science, 50(12),3315–3322.

8. Duraisamy, R., Mohan Kumar, S., Rajesh Kannan, A., Siva Shanmugam, N., & Sankaranarayanasamy, K. (2019). Reliability and sustainability of wire arc additive manufactured plates using ER 347 wire-mechanical and metallurgical perspectives. Proceedings of the Institution of Mechanical Engineers, Part C: Journal of Mechanical Engineering Science, 0954406219861136.

9. Gupta, A., Singh, H., & Aggarwal, A. (2011). Taguchi-fuzzy multi output optimization (MOO) in high speed CNC turning of AISI P-20 tool steel. Expert Systems with Applications, 38(6), 6822–6828.

10. Li, J. L. Z., Alkahari, M. R., Rosli, N. A. B., Hasan, R., Sudin, M. N., & Ramli, F. R. (2019). Review of wire arc additive manufacturing for 3d metal printing. International Journal of Automation Technology, 13(3), 346–353.

11. Li, Y., Han, Q., Zhang, G., & Horváth, I. (2018). A layers-overlapping strategy for robotic wire and arc additive manufacturing of multi-layer multi-bead components with homogeneous layers. International Journal of Advanced Manufacturing Technology, 96(9–12), 3331–3344.

12. Liu, W., Jia, C., Guo, M., Gao, J., & Wu, C. (2019). Compulsively constricted WAAM with arc plasma and droplets ejected from a narrow space. Additive Manufacturing, 27, 109–117.

13. Mandal, N., Doloi, B., Mondal, B., & Das, R. (2011). Optimization of flank wear using Zirconia Toughened Alumina (ZTA) cutting tool: Taguchi method and Regression analysis. Measurement: Journal of the International Measurement Confederation, 44(10), 2149–2155.

14. Michel, F., Lockett, H., Ding, J., Martina, F., Marinelli, G., & Williams, S. (2019). A modular path planning solution for Wire + Arc Additive Manufacturing. Robotics and Computer-Integrated Manufacturing, 60, 1–11.

15. Müller, J., Grabowski, M., Müller, C., Hensel, J., Unglaub, J., Thiele, K., Kloft, H., & Dilger, K. (2019). Design and parameter identification of wire and arc additively manufactured (WAAM) steel bars for use in construction. Metals, 9(7).

16. Park, J. S., Park, J. H., Lee, M. G., Sung, J. H., Cha, K. J., & Kim, D. H. (2016). Effect of Energy Input on the Characteristic of AISI H13 and D2 Tool Steels Deposited by a Directed Energy Deposition Process. Metallurgical and Materials Transactions A: Physical Metallurgy and Materials Science, 47(5), 2529–2535.

17. Rathod, C. H. A. N. D. A. R., and GONDI KONDA Reddy. "Experimental investigation of angular distortion and transverse shrinkage in CO2 arc welding process." International Journal of Mechanical Engineering, 5 (4), 21 28 (2016).

18. *Reddy, K. Srinivasulu. "Optimization & prediction of welding parameters and bead geometry in submerged arc welding." International Journal of Applied Engineering Research And Development 3.3 (2013): 1-6.*
19. *Rodrigues, T. A., Duarte, V., Miranda, R. M., Santos, T. G., & Oliveira, J. P. (2019). Current status and perspectives on wire and arc additive manufacturing (WAAM). Materials, 12(7).*
20. *Rosli, N. A., Alkahari, M. R., Ramli, F. R., Maidin, S., Sudin, M. N., Subramoniam, S., & Furumoto, T. (2018). Design and development of a low-cost 3d metal printer. Journal of Mechanical Engineering Research and Developments, 41(3), 47–54.*
21. *Ryan, E. M. (2018). On Wire and Arc Additive Manufacture of Aluminium. University of Surrey.*
22. *Samir Khan, M., Kumar, V., Mandal, P., & Chandra Mondal, S. (2018). Experimental Investigation of Combined TIG-MIG Welding for 304 Stainless Steel Plates. IOP Conference Series: Materials Science and Engineering, 377(1).*
23. *SALUJA, RATI, and K. M. Moeed. "Depiction of detrimental metallurgical effects in grade 304 austenitic stainless steel arc welds." International Journal of Mechanical and Production 8.6 (2018): 207-218.*
24. *Seow, C. E., Coules, H. E., Wu, G., Khan, R. H. U., Xu, X., & Williams, S. (2019). Wire + Arc Additively Manufactured Inconel 718: Effect of post-deposition heat treatments on microstructure and tensile properties. Materials and Design, 183, 108157.*
25. *Spencer, J. D., Dickens, P. M., & Wykes, C. M. (1998). Rapid prototyping of metal parts by three-dimensional welding. Proceedings of the Institution of Mechanical Engineers, Part B: Journal of Engineering Manufacture, 212(3), 175–182.*
26. *Xiong, J., Li, Y., Li, R., & Yin, Z. (2018). Influences of process parameters on surface roughness of multi-layer single-pass thin-walled parts in GMAW-based additive manufacturing. Journal of Materials Processing Technology, 252, 128–136.*
27. *Xu, F., Dhokia, V., Colegrove, P., McAndrew, A., Williams, S., Henstridge, A., & Newman, S. T. (2018). Realisation of a multi-sensor framework for process monitoring of the wire arc additive manufacturing in producing Ti-6Al-4V parts. International Journal of Computer Integrated Manufacturing, 31(8), 785–798.*